HEFAT2014
10th International Conference on Heat Transfer, Fluid Mechanics and Thermodynamics
14 – 16 July 2014
Orlando, Florida

INVESTIGATION INTO USING LIQUID CRYSTAL THERMOGRAPHY FOR MEASURING HEAT TRANSFER COEFFICIENTS AND WALL TEMPERATURE PROFILES AT INLETS AND UNDERDEVELOPED REGIONS

Van der Westhuizen J E, Dirker J*, Meyer J P
*Author for correspondence
Department of Mechanical and Aeronautical Engineering,
University of Pretoria,
Pretoria, 0002,
South Africa,
E-mail: jaco.dirker@up.ac.za

ABSTRACT

In this paper the wall surface temperature distributions at the inlet regions of a tube-in-tube counter flow heat exchanger were investigated by making use of Liquid Crystal Thermography (LCT). With flow not being fully developed at the inlet region it is difficult to predict the heat transfer coefficient and the appropriate wall temperature on the inner tube under different flow conditions. In this study water was considered in the annulus in the turbulent flow with annular Reynolds numbers of 1 000, 5 000 and 10 000. Local annular heat transfer coefficients were determined from the measured wall temperature profiles and the derived local annular bulk fluid temperatures based on the measured coupled local heat transfer rate in the inner tube. It was found that Liquid Crystal Thermography allowed for the measurement of the average wall temperature which could vary significantly in the inlet region. It was also found that the local heat transfer coefficients varied within a large extent. For the particular heat exchanger under investigation here which had annular diameters of 36 mm and 19.5 mm, heat transfer coefficients reached a maximum from 150 mm onwards after the inlet.

INTRODUCTION

Heat transfer coefficients for the inlet and underdeveloped regions of heat exchangers are not covered well by literature. Total or average heat transfer and heat transfer coefficients are often the topics of discussion, leaving localized results unpublished or un-investigated. Even literature covering the average or total heat transfer coefficients is often conflicting. Dirker and Meyer [1] studied existing literature based on experimental data for concentric tube-in-tube heat exchangers and found differences of up to 20 % between the different literature sources. These discrepancies may also be expected for other types of heat exchangers as well, and can be linked to how results are presented and whether the heat transfer in the inlet regions were or not in terms of the relative inlet length compared to the total

NOMENCLATURE

A	[m^2]	Area
C_p	[J/kg.K]	Specific heat
CV	[-]	Control volume
D	[m]	Diameter
D_h	[m]	Hydraulic Diameter
HSV	[-]	Hue, Saturation, Value colour system
h	[W/m^{2}K]	Convective heat transfer coefficient
k	[W/mK]	Thermal conductivity
$\dot{m}$	[kg/s]	Mass flow rate
Nu	[-]	Nusselt number
$\dot{Q}$	[W]	Heat transfer rate
RGB	[-]	Red, Green, Blue colour system
Re_o	[-]	Reynolds number,
t_{resin}	[t]	Reisn layer thikness
T	[°C]	Temperature
$\bar{T}$	[°C]	Average temperature
V	[m/s]	Fluid velocity
x	[m]	Axial length along the heat exchanger
Greek symbols:		
δ_{Nu}	[%]	Uncertainty in the Nusselt number
μ	[m^2/s]	Kinematic viscosity
ρ	[kg/m^3]	Density
ϕ	[rad] or [°]	Angular position
Subscripts:		
b		Bulk property
h		Based on hydraulic diameter
i		Inner tube
i,in		Inner tube inlet
i,out		Inner tube outlet
j		CV index number
$local$		Local property
o		Annulus
o,in		Annulus inlet
o,out		Annulus outlet
$resin$		Resin layer
w		Inner tube outer wall

tube length. Well known correlations such as those developed by Gnielinski [2] for the full length of the heat exchanger do not specifically give attention to the inlet and underdeveloped regions.

In recent studies done by our research group which included the determination of local heat transfer coefficients [3] , it was found that even for long heat exchangers, the flow seldom becomes thermally fully developed and that heat transfer coefficients close to inlets are significantly higher than the averaged heat transfer coefficients described by most correlations. This trend is also covered in Cengel's book [4] where it is shown that the heat transfer capability increases with a logarithmic form as one moves closer to the inlet of the heat exchanger. This theoretical trend was also shown to occur by Maranzana *et al* [5] for mini and micro channels.

Reliable local wall temperatures are needed in order to obtain accurate local heat transfer characteristics. This in turn is needed in order to obtain a good understanding of the heat transfer to be expected from a heat exchanger. With this information, it is possible to design efficient and cost effective heat exchangers.

It is, however, difficult to measure wall and bulk fluid temperatures in the inlet regions to determine localised heat transfer coefficients. Using large numbers of thermocouples to measure the surface temperature distributions are not suitable since the thermocouple leads significantly disrupt the flow of the medium. For this reason, alternative experimental techniques need to be considered.

The technique of using Thermo-chromic Liquid Crystals (TLC) to measure surface temperatures is called Liquid Crystal Thermography (LCT). TLCs change their reflected colour as a function of their temperature when viewed in the presence of white light [6]. A temperature uncertainty of 0.22°C was claimed by Tam and Ghajar [7] while using this technique to investigate micro channel heat transfer. They considered a wide range of TLCs and covered a bandwidth of 20°C, similar to what was used in this paper. Heat transfer research has also been undertaken with the aid of TLC by Stasiek and Kowalewski [8]. They used water as their working fluid measuring surface temperatures, fluid temperatures and flow velocities. TLC particles were also used by Li *et al.* [9] to investigate natural convection in a cubic cavity by suspending temperature sensitive particles in a glycerol-water mixture.

By treating a tube surface with a TLC impregnated paint it is possible to obtain a complete surface temperature map by covering the whole circumference of a tube at the inlet and underdeveloped regions of the heat exchanger. Local regions of increased or decreased heat transfer rates may be identified using these temperature maps. An advantage of using LCT is that it is a less intrusive measuring method than thermocouple measurement.

PURPOSE OF STUDY

In this study a methodology was developed for using LCT in a tube-in-tube heat exchanger to obtain surface wall temperatures and localized heat transfer coefficients in the annular passage close to the inlet. The feasibility of using TLC for this application was investigated since little information about TLC usage with tube-in-tube heat exchangers could be found in literature. In principle the technique described in this paper could also be used on a number of other heat exchanger geometries.

EXPERIMENTAL FACILITY

Figure 1 gives the layout of the experimental test facility, showing all components. The experimental facility consisted of two closed loop systems. The first loop contained a water heater with a reservoir and the second contained a chiller also with a tank. Table 1 lists all the equipment with a brief explanation of each. Either one of the loops could be connected to either the annulus or the inner tube. This facilitated testing either heating or cooling of the annulus. However, only cooled annular cases are considered in this paper.

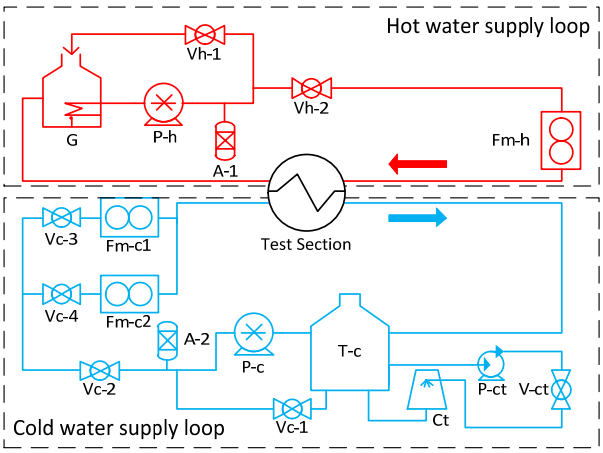

Figure 1 Experimental test facility layout

Table 1 List of experimental facility equipment

Hot water supply loop		**Cold water supply loop**	
G	Geyser, 12 kW 600 liters	T-c	Cold water tank, 1000 liters
Vh	Ball valves	P-ct	Chiller pump
P-h	Positive displacement pump	V-ct	Chiller valve
A-1	4 *l* accumulator	Ct	Chiller, 16 kW
Fm-h	Coriolis flow meter, 54.5 – 1090 *l*/h	P-c	Positive displacement pump
		A-2	4 *l* accumulator
		Vc	Ball valves
		Fm-c1	Coriolis flow meter, 54.5 – 1090 *l*/h
		Fm-c2	Coriolis flow meter, 4.1 – 82 *l*/h

TEST SECTION

Figure 2 shows a section view of the counter-flow heat exchanger test section consisting of three concentric tubes (also refer to Figure 3). Tube 1, constructed from Perspex, had an inner diameter of $D_0 = 36$ mm and acted as the outer wall of the annulus. The see-through Perspex facilitated capturing images of the inner wall (tube 2) of the annulus which were treated with TLC's to obtain the inner wall temperature profiles. Tube 2, constructed from copper, had an outer diameter of $D_1 = 19.5$ mm and had a wall thickness of 0.8 mm which included all the LCT surface paint layers (these will be discussed shortly). The TLC had an activation temperature of 20°C with a range of 20°C. Tube 2 was concentrically located inside tube 1 by means of flanged connections on either side. Tube 3, the inner most tube, had an outer diameter of $D_3 = 6.5$ mm and was used to measure the change in the bulk fluid temperature of the water passing through tube 2 (referred to in this paper as the inner fluid).

Tube 3 was fully emerged in the center of tube 2 and was surrounded by the inner fluid. It was kept concentric within tube 2 by means of radial spacers and contained 11 measuring stations along its length with the thermocouple leads passing through its inside. Each measuring station was constructed from short (15mm long) sections of copper tube onto which two T-type thermocouples were soldered internally (see Figure 4 for an enlargement). The measuring stations were separated from each other by 95 mm long acrylic tube sections having the same outer diameter as the copper sections. The acrylic sections minimized axial thermal conduction along the measuring tube, ensuring that the temperature measured at each measuring station was that of the fluid temperature in the center of tube 2, at that location. The temperatures measured by the measuring tube 3 were used to determine the change in the bulk fluid temperature inside tube 2.

In order to treat the outer surface of tube 2, three layers of cover was needed: first a black paint layer, then the TLC's and lastly a thin clear resin layer to protect the TLC's from the water, all of the layers together had a thickness of $t_{resin} = 0.25$ mm (the resin layer contributed the most). The first two layers were applied using a custom constructed air-brush painting facility which allowed for an even and repeatable paint distribution and paint layer thickness. The epoxy layer was applied while tube was continually rotated to produce an even distribution of this layer. Once cured, the outer layer was checked for circularity and sanded smooth.

The inlet and outlet of the annulus were orientated perpendicularly to the annular flow direction and were located on the upper side of the heat-exchanger. Each inlet and outlet had an inner diameter of 16 mm and was axially 945 mm apart (centre-to-centre). The total heat excange length was 1001 mm long, of which 320 mm were investigated using the liquid crystal coated portion of tube 2.

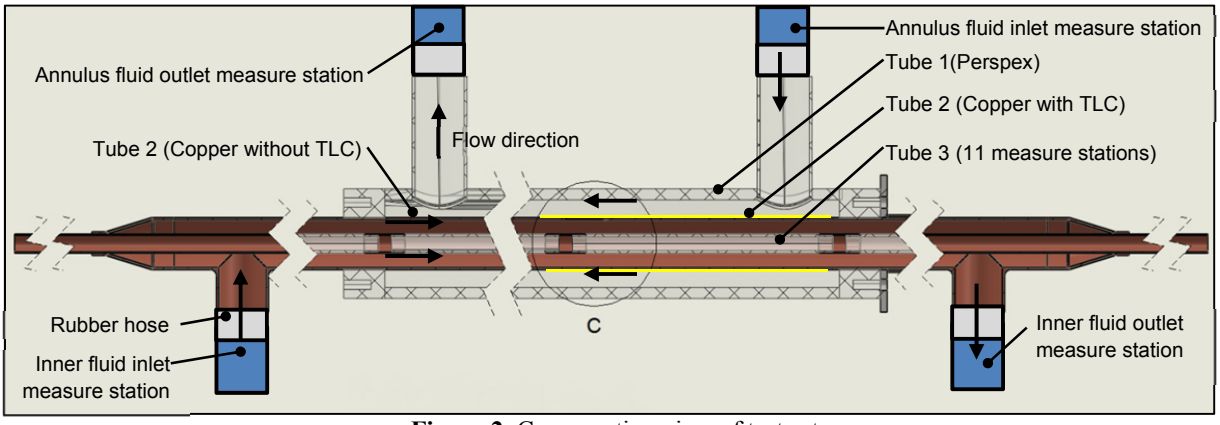

Figure 2 Cross section view of test setup

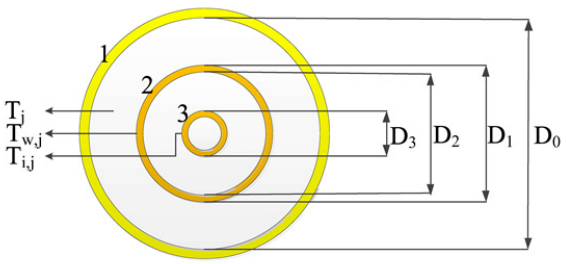

Figure 3 Diameter definitions of concentric tubes

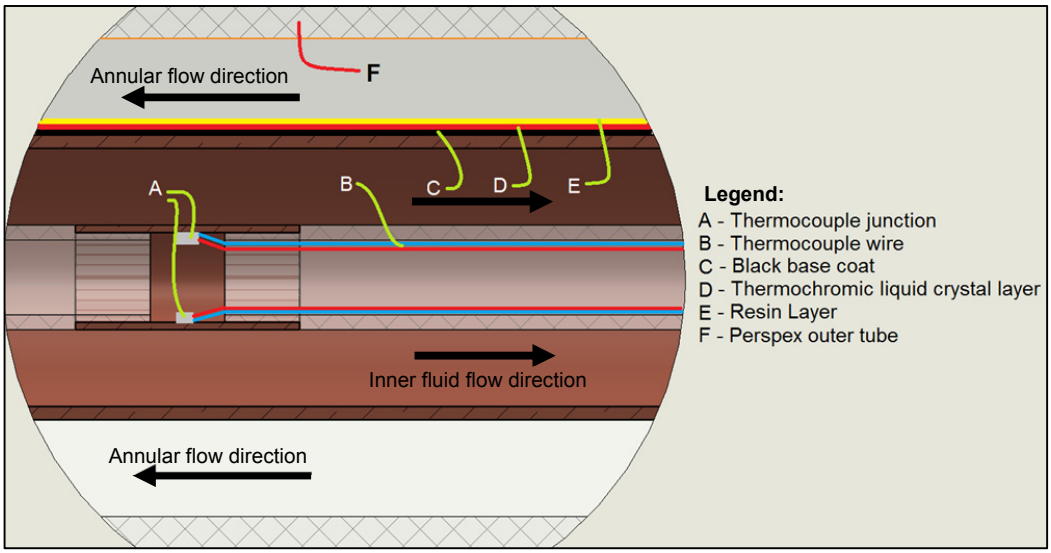

Figure 4 Detailed section view of test setup (detail C)

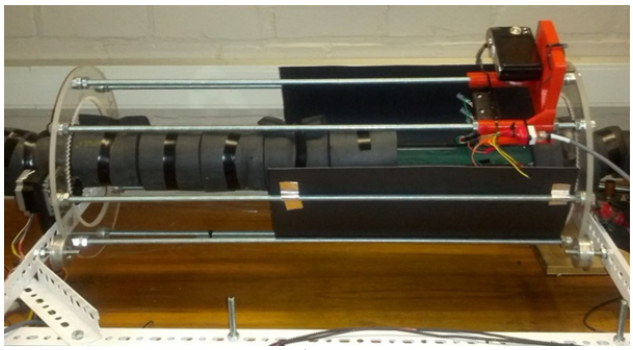

Figure 5 Rotating camera setup

Thermal insulation was placed around the outside heat exchanger to limit heat loss or gain from the laboratory. Only that portion that was being imaged was uncovered temporarily. Figure 5 shows the setup used to capture the images of the LCT treated portion of tube 2. The camera mounting (red) was rotated concentrically around the heat exchanger through 360°, taking images at pre-determined angular positions. The angular position of the camera was adjusted by a stepper motor controlled via a PC console.

Images were captured via a 7 megapixel digital camera of which the light-exposure could be controlled. Light was supplied by intensity controlled LEDs which had a fixed relative position relative to the camera. After one rotation of the camera around the heat exchanger was completed, the camera was moved along the heat exchanger length and the next ring of images could be captured.

Bulk fluid temperatures at the inlets and outlets of the heat exchanger (for the annular fluid and the inner fluid) were measured at measuring stations directly before or after the heat exchanger (refer to Figure 2). Each measuring station consisted of a copper tube portion with 4 thermocouples connected to it. The measuring stations were separated from the heat exchanger by means of flexible hoses to reduce inaccuracies due to axial conduction. All inlet and outlet measuring stations were preceded by a 90° elbow, acting as a mixing station. All thermocouples were calibrated against a Pt100 with a manufacturer specified uncertainty of 0.01°C. A 3rd order regression fit was used to correct raw thermocouple data into calibrated thermocouple data.

EXPERIMENTAL PROCEDURE

The heat exchanger was tested for a variety of inlet temperatures as well as flow rates for a heated and cooled annulus respectively. However, only data for a cooled annulus is reported on in this paper. Data sub-sets were only sampled when the heat exchanger was operating in steady operating conditions. Steady state was defined as follows: when the inlet to outlet temperature difference stayed within a 0.1°C band for both the inner tube and the annulus over 2 minutes. Thermocouple data were captured for the entire time in which the heat exchanger was operational. Since about 14 minutes were needed to capture the surface images of tube 2, it was required to analyse the temperature changes over time to identify weather the heat exchanger was in fact operating in steady state conditions for the entire duration. It was found that due to routine adjustments of the heating and cooling loops, it was more often than not, impossible to maintain pure steady states over the 14 minute duration.

To counter this, an approach was used where the temperature and LCT images were captured in seven sub-sets (one for each rotational cycle of the camera) and analysed individually before combining the data. It was

found that steady state conditions were easily obtained in the shortened time duration needed to capture one sub-set.

Figure 6 shows the temperature variations over time for an arbitrary test configuration where the annular Reynolds number was $Re_o = \rho V D_h/\mu = 1\,000$. The hydraulic diameter is based on the inner and outer annular wall diameters: $D_h = D_0 - D_1$. When analysing the heat transfer characteristics for the image set taken in ring 1 (as will be discussed later), the thermocouple data were taken for that specific time duration being approximately minutes 0 to 2. When the image set was recorded for the second ring, temperature data for approximately minutes 3 to 4 were used etc.

Next, all the images were captured around and along the length of the heat exchanger while all external light sources to the laboratory was removed and the laboratory was in darkness except for the LED light source. For each axial position, the camera was rotated around the heat exchanger and two images were collected at each location. After completing one revolution the camera was moved axially through a distance of 40 mm and the process was repeated until the whole testing length was covered. After a full data set was collected for a specific inlet temperature and flow rate scenario, the flow rate and/or inlet temperatures were changed and all the steps above were repeated. Recursively completing these steps resulted in an array of data relating to different Reynolds numbers and inlet temperatures in the annulus.

DEFINITIONS

Figure 7 gives a schematic representation of the test section and positions of the 11 equally space temperature measuring stations along the length of the heat exchanger, resulting in 10 control volumes (CV) which were used to analyze the data. Figure 7 also designates the temperature nomenclature. T_j refers to the bulk fluid temperature in the annulus at measuring station j. $T_{w,j}$ is the wall temperature of tube 2 measured using the TLC's. $T_{i,j}$ refers to tube 3's, temperature probe measurement at station j.

DATA REDUCTION

The wall surface temperatures on tube 2 were extracted from the still images of the TLCs captured by the camera. In order to determine local heat transfer coefficients, the average circumferential tube wall temperature at a particular axial location was needed. The conversion of the normal RGB (Red, Green and Blue) values for each of the pixels generated by the camera to the HSV (Hue angle, Saturation and Value) color system was done by using a built in function of Matlab, rgb2hsv. For more information on the conversion process, please refer to the book by Moeslund [10].

The hue angle represents the color of the pixel and is not influenced by the brightness of the pixel. This aided in consistent readings. Hue angle values were assigned to certain temperature values. This process was similar to calibrating a thermocouple, but instead of logging a voltage reading, a hue angle "reading" was recorded.

A Calibration test was conducted on the liquid crystal batch purchased, then repeated on the heat exchanger after the TLC were applied to tube 2 before test runs.

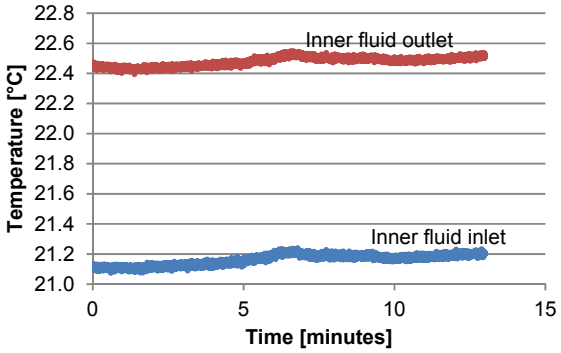

Figure 6 Inlet and outlet temperature variations

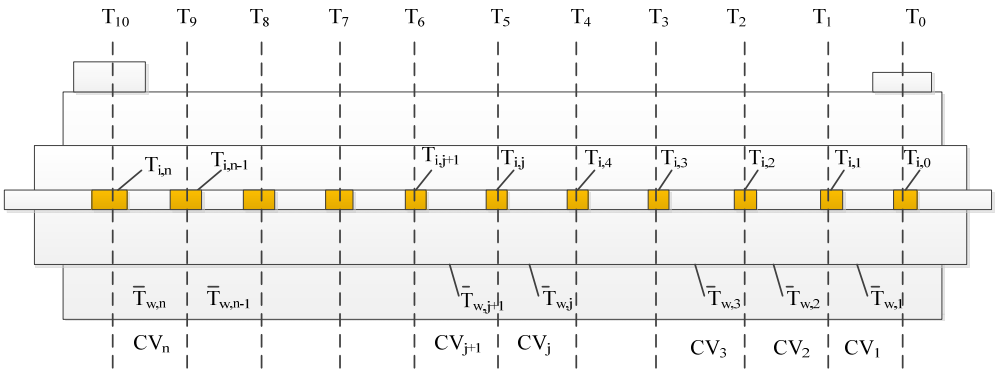

Figure 7 Designation of control volumes and temperatures

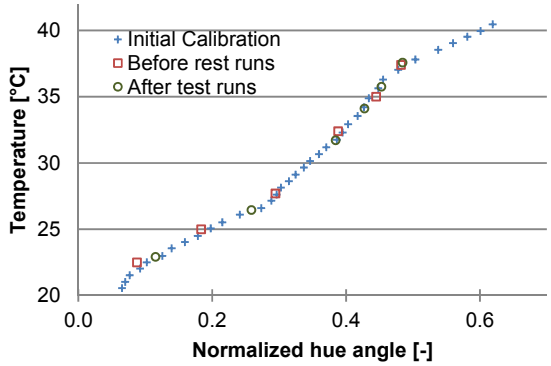

Figure 8 Liquid Crystal calibration curve

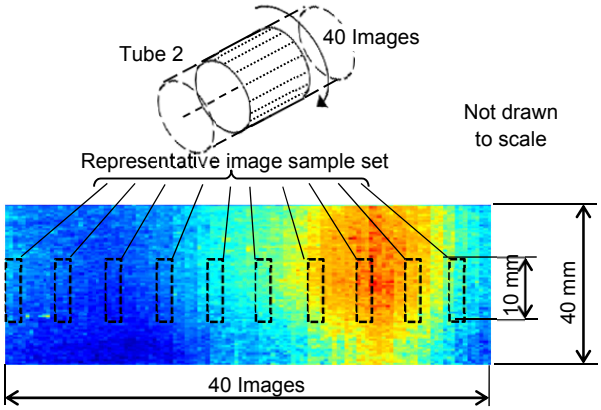

Figure 9 Temperature profile obtained for one "ring" with extracted regions shown

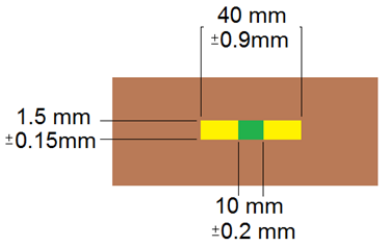

Figure 10 Dimension inaccuracies due to light refraction

Calibration was repeated after test runs were completed to ensure that the crystals were still performing predictably. Figure 8 gives the calibration data for the TLC's used in this study in terms of the normalized hue angle as calculated from the Matlab rgb2hsv function divided by 360° (since the hue angle ∈ [0,360]). A six order polynomial fit was used to facilitate converting the measured hue angle into a temperature for each extracted pixel. Over the surface of the tube a maximum scatter of 0.2°C was observed as per the manufacturer specifications.

Figure 9 shows a composite image created by using extracted temperatures from 40 images captured around the circumference of tube 2 covering a ring 40 mm wide. In this figure blue refers to colder surface temperatures, while red refers to warmer temperatures. By repeating this for 7 axial positions resulted in 280 images which could be stitched together to produce a composite image of a surface roughly 300 mm long by 60 mm circumferentially. Since the incident and reflection angles of light affect the recorded hue angle, only a strip measuring 10 mm wide was used such that the viewing angle of the portion of tube surface that is represented was perpendicular (within 2°) to the surface. This also limited any affect that refraction might have. Figure 10 shows the expected dimensional inaccuracies using Snell's law of light refraction through the Perspex and water interfaces.

In order to speed up the testing procedure, to remain within a steady state window, only 10 recording positions was used around the circumference. The difference in the average surface temperature due to fewer images were investigated and it was found to be less than 0.04°C when comparing the average surface temperature based on 40 images to that when 10 images were used. It was therefore concluded that 10 photos around the circumference gave a representative value of the average surface temperature of the heat exchanger for that specific axial position.

By using the inner fluid bulk temperatures obtained from the measuring stations in tube 3, it was possible to examine the amount of heat transferred in each of the control volumes shown in Figure 7. This is given as:

$$\dot{Q}_{i,j} = \dot{m}_i C_p (T_{i,j} - T_{i,j+1}) \qquad (1)$$

To maintain the energy balance, the amount of heat gained or lost by the inner fluid must be the same as the amount of heat lost or gained by the annular fluid:

$$\dot{Q}_{o,j} = \dot{Q}_{i,j} \qquad (2)$$

This was used to predict the bulk fluid temperature in the annulus at the boundary of the next control volume:

$$\dot{m}_o C_p \left(T_{o,j} - T_{o,j+1}\right) = \dot{m}_i C_p (T_{i,j} - T_{i,j+1}) \qquad (3)$$

In the above equation, the only unknown is T_{j+1}, since all preceding annular bulk fluid temperatures can already be expressed in terms of the annular bulk inlet fluid temperature. To obtain the local heat transfer coefficients (for the particular control volume), the following equation may be used:

$$\dot{Q}_j = h_j A_j \left(\bar{T}_{w,j} - \bar{T}_{o,j}\right) \qquad (4)$$

With: $$\bar{T}_{o,j} = \frac{T_{o,j} + T_{o,j+1}}{2} \qquad (5)$$

And: $$\bar{T}_{w,j} = \frac{1}{A} \iint_A T(\phi, x) dA + \frac{\dot{Q}_{o,j} t_{resin}}{k_{resin} A_j} \qquad (6)$$

The temperature field $T(\phi,x)$ was obtained from the TLC layer on tube 2 of the heat exchanger. The last term in Eqn. (6) includes the effect of the thermal resistance of the epoxy layer between the TLC layer and the water in the annulus. Since the epoxy layer was thin, a linear one-dimensional approximation was used. The thermal conductivity of the epoxy used in this study was measured to be 0.22 W/mK. The local Nusselt number could then be calculated using:

$$Nu_{local,j} = \frac{h_j D_h}{k_j} \qquad (7)$$

All the thermo physical properties of water (specific heat, density and thermal conductivity) used in these analyses were obtained from the formulas put forward by Popiel and Wojtkowiak [11]. The formulas have a low uncertainty for the temperature range between 0 and 150°C for liquid water.

UNCERTAINTY ANALYSIS

As with all instrumentation, measurements are not exact. In this section a brief overview of the uncertainties are discussed.

The method used to determine the uncertainties of the calculated results are described by Kline and McClintock [12]. The result of this method gives an uncertainty in the same units as what the calculated results are. Therefore, for one of the measuring stations inside the inner tube, the uncertainty of the measured temperature is ±0.078°C. The value is then (within a 95% confidence based on a measured value of 20°C).

Table 2 shows a higher uncertainty (0.76°C) for the TLC's. This is due to the manufactured specified uncertainty being 0.22°C, the PT 100 used to calibrate against having an uncertainty of 0.01°C and the maximum deviation from the six order polynomial curve fit. This results in the 0.76°C uncertainty for a single extracted pixel. This uncertainty was, however, diminished due to the sheer number of pixels used in calculating the average surface temperature for one of the rings. The total number of pixel clusters used per ring is 600. Therefore, the resultant uncertainty becomes smaller than 0.1°C. The uncertainty of the Nusselt number, δ_{Nu}, (Table 3) was also calculated using the method of Kline and McClintock.

The large uncertainties for the local Nusselt number are due to the accuracy with which one is able to measure the bulk temperature change of the inner fluid to obtain the heat transfer rate. Although the uncertainty of the local temperature measurements within tube 3 is low (0.078°C), the temperature change between two adjacent stations are relatively small and can be as low as 0.11°C when the annular flow rate is low. The heat transfer uncertainty per control volume is therefore the quantity contributing most to the Nusselt number uncertainty.

Table 2 Uncertainties of equipment used

Equipment	Range	Uncertainty
Thermocouple	-200 – 350 °C	0.11°C
TLC's	20 – 41 °C	0.76°C
Flow meter	0.015 – 0.603 kg/s	0.11% of reading

Table 3 Nusselt number and surface temperature uncertainties for different annular Reynolds numbers

Re_o	δ_{Nu}	$\overline{T_w}$
1 000	206%	±0.03°C
5 000	105%	±0.03°C
10 000	99%	±0.03°C

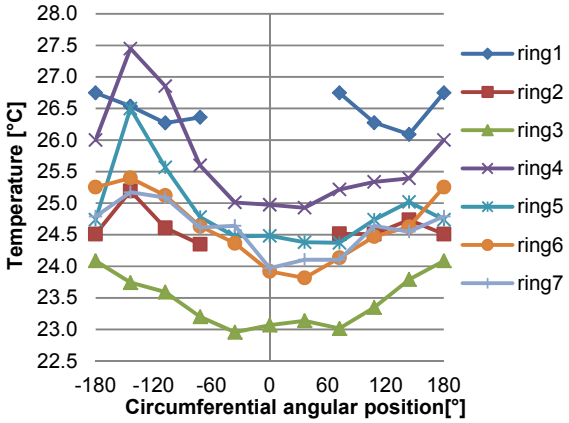

Figure 11 Circumferential TLC temperature distribution for each ring (Re_o = 1 000)

RESULTS

Some preliminary results are presented in this section.

TLC temperature field

It was found for the case with Re_o equal to 5 000 there is temperature variations of up to 8.2°C between the warmest and coldest positions on Tube 2.

Figure 9 shows an example of temperature gradients obtained using the TLC's on tube 2 for one ring only. These values have not yet been adjusted to take the thermal resistance of the resin layer into account. It can be seen that there is a significant temperature variation on the surface that will be difficult to measure with thermocouples. Based on the 10 mm wide section of the ring, the local wall temperatures for each ring is given in Figure 11.

It can be seen that temperature distributions around the circumference of the tube (with 0° referring to upper point of the tube) were not necessarily symmetrical. Each of the values given is based on the average hue angle measured within a portion of each image that responded to the region that was directly in line with the camera. Ring 1 corresponds to the inlet of the annular flow passage. Because of the annulus inlet, this ring is only partially recorded.

Ring 3 demonstrated the lowest TLC temperatures of all the rings in all test cases that were conducted. From distributions like the one shown in Figure 9 the average TLC temperature for each ring were determined and used to calculate the averaged heat transfer coefficient for the different control volumes.

Heat transfer coefficients

Three cooled annulus cases at annular Reynolds numbers of 1 000, 5 000 and 10 000 will be discussed here. For each case an inner fluid Reynolds number of 3 700 was used (inner flow rate of 0.06653 kg/s and also based on the hydraulic diameter of the inner tube). The inner Reynolds number was based on the hydraulic diameter of the inner flow passage. It was chosen sufficiently high to allow for significant fluid mixture within tube 2 such that the measuring stations on tube 3 could be used to obtain the inner fluid bulk temperature but still maintaining a high temperature difference between subsequent measuring stations.

For an annulus Reynolds number of 10 000, the local bulk fluid temperatures measured in tube 2, as well as the deduced bulk fluid temperature in the annulus using Eqn. (3) are shown in Figure 12 along the axial direction of the inlet region. Figure 13 repeats the bulk fluid temperatures, but also gives the measured local averaged TLC temperatures and the heat transfer surface wall temperatures. It can be seen that the thermal resistance of the resin epoxy has a significant effect, even if the epoxy layer is thin. Thus, care has to be taken when measuring the thermal conductivity of the resin. It could be noted that there was a disturbance in the wall temperature at about 150 mm from the inlet. This was checked for repeatability and it was found to occur for all flow rate cases, as well as for different test sections.

The information in Figure 12 and Figure 13 represent a snapshot of the bulk fluid temperature and surface temperature distribution, and would look different if either the annulus or inner fluid inlet temperatures changed slightly. As mentioned earlier, it was difficult to maintain steady state conditions for the entire duration of time that was needed to record the wall surface temperatures. If slight variations in the inlet conditions occurred during the recording period it was needed to update the local wall surface and bulk fluid temperatures before the local heat transfer coefficients were calculated.

Figure 14 shows the calculated heat transfer coefficients for the three Reynolds number values. It can be seen that the heat transfer coefficients changed dramatically from position to position close to the inlet region of the heat exchanger. The peak heat transfer coefficient was found to occur from 150 mm onwards from the inlet of the annulus for this particular heat exchanger.

The variation in the local wall temperature is indicative of a fluctuation in the local heat transfer rate and/or an improvement in the mixing phenomenon and thus a higher heat transfer coefficient influenced by the inlet flow velocity distribution due to the flow not being fully developed. Further investigation is needed to determine what the cause of this was.

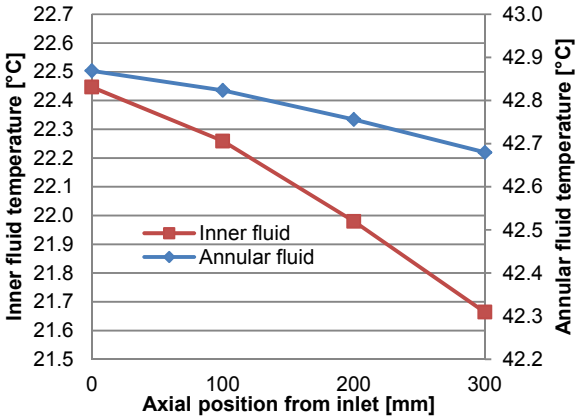

Figure 12 Bulk fluid temperatures (for Re_o =10 000)

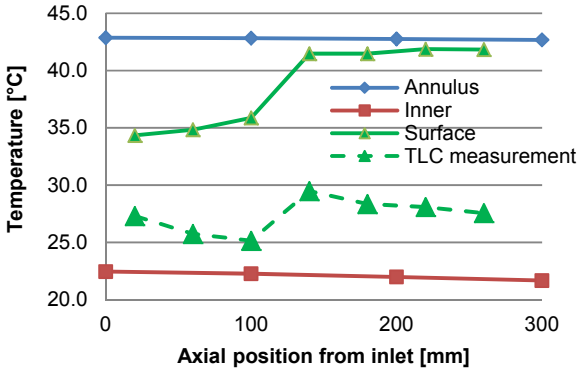

Figure 13 Temperature distribution at inlet (Re_o = 10 000)

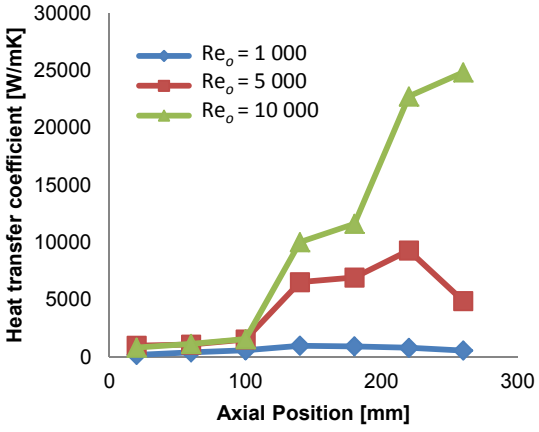

Figure 14 Averaged local heat transfer coefficients

CONCLUSION

The inlet region of a tube-in-tube heat exchanger was investigated by using LCT to obtain the local wall surface temperatures. A method with which the wall temperature of the heat transfer tube can be obtained using LCT was proposed and used to determine the profile of the heat transfer coefficient in the undeveloped region directly after the annulus inlet.

Initial results indicate that the TLC's have sufficient temperature response with which local temperature profiles can be obtained and it was shown that these experimental techniques can be used to obtain local heat transfer coefficients. It was found that there is a significant change in the heat transfer coefficient at the inlet that could be attributed to flow velocity distributions caused by the inlet jets.

Care should however be taken when measuring the fluid temperature change as the accuracy of this reading influences the uncertainties by a large margin. In principle the technique described in this paper could also be used on a number of other heat exchanger geometries.

REFERENCES

[1] J. Dirker and J. P. Meyer, "Convection heat transfer in concentric annuli", *Experimental heat and mass transfer,* vol. 17, pp. 19-29, 2004.

[2] V. Gnielinski, "Heat transfer coefficients for turbulent flow in concentric annular ducts", *Heat transfer engineering,* vol. 30, pp. 431-436, 2009.

[3] W. R. v. Zyl, J. Dirker, and J. P. Meyer, "Single-phase convective heat transfer and pressure drop coefficients in concentric annuli", *Heat transfer engineering,* vol. 34, pp. 1112-1123, 06 Feb 2013 2013.

[4] Y. A. Cengel, *Heat and mass transfer*, Third ed. New York: Mc Graw Hill, 2006.

[5] G. Maranzana, I. Perry, and D. Maillet, "Mini- and micro-channels: influence of axial conduction in the walls", *International journal of heat and mass transfer,* vol. 47, 2004.

[6] C. Camci, *Introduction to liquid crystal thermography and a brief review of past studies*.

[7] L. M. Tam, H. K. Tam, A. J. Ghajar, and W. S. NG, "Heat transfer measurements for a horizontal micro-tube using liquid crystal thermography", in *International symposium on heat transfer and energy conservation*, 2012, pp. 62-66.

[8] J. A. Stasiek and T. A. Kowalewski, "Thermochromic liquid crystals applied for heat transfer research", *Opto-electronics review,* vol. 10, pp. 1-10, 2002.

[9] H. Li, C. Xing, and M. J. Braun, "Natural convection in a bottom-heated top-cooled cubic cavity with a baffle at the median height: experiment and model validation", *Heat Mass Transfer,* vol. 43, pp. 895-905, 2007.

[10] T. Moeslund, *Introduction to video and image processing*. New York: Springer, 2012.

[11] C. O. Popiel and J. Wojtkowiak, "Simple formulas fo thermophysical properties of liquid water for heat transfer calculations", *Heat transfer engineering,* vol. 19, pp. 87-101, 1998.

[12] S. Kline and F. McClintock, "Describing uncertainties in single-sample experiments", *Mechanical engineering,* vol. 75, pp. 2-8, 1969.